Biophysical Characteristics of ATH434, a Unique Iron-Targeting Drug for Treating Friedreich's Ataxia

Ashley E. Pall [1], Silas Bond [2], Margaret Bradbury [2], Andrew M. Lipchik [1], Timothy L. Stemmler [1]
[1] Department of Pharmaceutical Sciences, Wayne State University, Detroit, MI 48201 USA
[2] Alterity Therapeutics, Melbourne, Victoria, 3000 Australia

Objective

- Characterize iron-drug complexes, including ATH434, as potential Friedreich's Ataxia treatments
- Differentiate traditional iron chelators and novel iron-targeting compounds based on their affinities and atomic-level interactions with Fe^{2+} and Fe^{3+}:

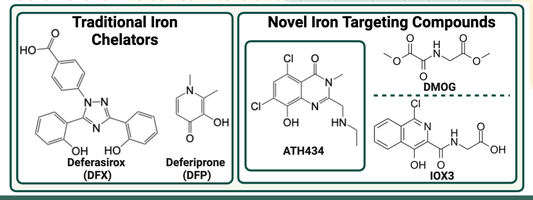

Introduction

Friedreich's ataxia (FRDA) is a fatal orphan-designated neuromuscular disorder with early age of onset and inadequate standard of care options. Structural variation within the FXN gene reduces intracellular levels of frataxin, a primarily mitochondrial protein that binds reactive Fe^{2+} with a moderate ~3uM affinity [1,2] similar to endogenous iron chaperone proteins [3]. Frataxin deficiency, in turn, impairs the mitochondria's ability to utilize Fe^{2+} in energy production. The concomitant toxic Fe^{2+} accumulation is a hallmark phenotype driving FRDA pathogenesis.

Figure 1: The pathophysiology of iron accumulation in Friedreich's Ataxia

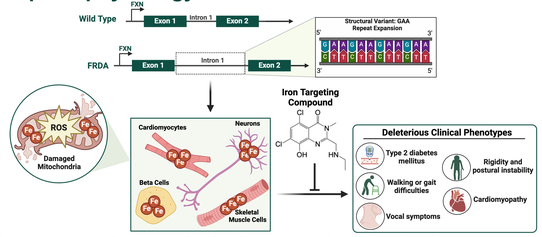

Iron chelation therapy has been a logical approach for reducing excess cellular iron. Traditional iron-chelating drugs however, have had limited clinical efficacy and exacerbate ataxia in severe cases of FRDA [4]. Therapeutic efficacy of traditional chelators may be limited by their exceptionally high affinity for non-pathogenic, ferritin-stored iron (Fe^{3+}), which in turn disrupts iron homeostasis [5,6]. Conversely, they may have inadequate interactions with Fe^{2+}, the species that underlies FRDA pathology. It's proposed that an improved iron targeting compound for FRDA should possess biophysical properties that mimic endogenous iron binding proteins such as frataxin, that both chaperones Fe^{2+} and shelters cells from Fe^{2+} induced ROS. Recently, novel iron targeting compounds, including ATH434 (in Phase 2 clinical trials for Multiple System Atrophy), have shown promising results in pre-clinical animal models for conditions associated with excess labile iron. A comprehensive evaluation of the biophysical properties of both traditional iron chelators and novel iron targeting compounds, however, is largely absent, underscoring a fundamental disconnect between therapeutic options and an understanding of clinical efficacy and adverse outcomes. The present results may provide a logical framework for evaluating novel iron targeting compounds, such as ATH434, in FRDA.

Methods

- **Fe^{2+} Competitive Binding Assays**: Conducted to measure Fe^{2+} binding affinity and performed within an anaerobic chamber, providing environmental conditions suitable for studying Fe^{2+} binding free of an external oxidant
- **Isothermal Titration Calorimetry:** Used to assess thermodynamic parameters for each complex including binding affinity and stoichiometry
- **X-ray Absorption Spectroscopy:** Data collection and analysis performed to deconvolute iron binding ligand identity

Fe^{2+} Binding Affinity

Figure 2: Measuring ATH434 Fe^{2+} chelation using metal competition assays with Mag-Fura-2. Representative UV-Vis spectra (left) of ATH434 competing with Mag-Fura-2 for Fe^{2+} in solution. Simulation of the data points using Dynafit (right) provide ATH434 affinity for Fe^{2+}.

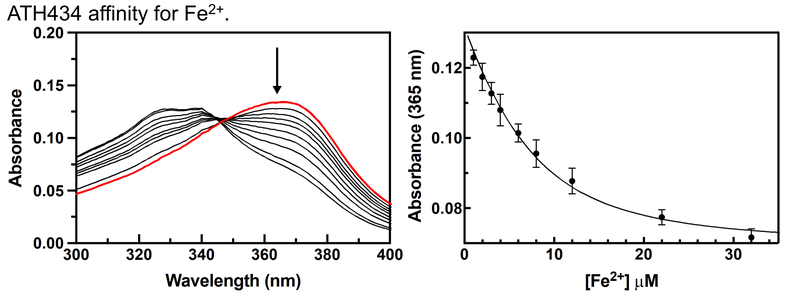

Table 1: Fe^{2+} binding affinities (n=3)

Drug	Deferasirox (DFX)	ATH434	Deferiprone (DFP)	DMOG	IOX3
K_d Value (µM)	4.25 ± 1.3	4.85 ± 1.1	15.2 ± 4.0	25.9 ± 8.1	32.7 ± 4.1

- The low µM affinities of ATH434 and DFX for Fe^{2+} are similar to those of frataxin and other endogenous iron chaperones
- DFP, DMOG, and IOX3 have weaker interactions

Thermodynamic Stability

Figure 3: Isothermal titration calorimetry (ITC) data of ATH434 measuring Fe^{2+} chelation. Representative figure of raw binding isotherm (left) with integrated thermogram (right) for Fe^{2+} titrated into ATH434.

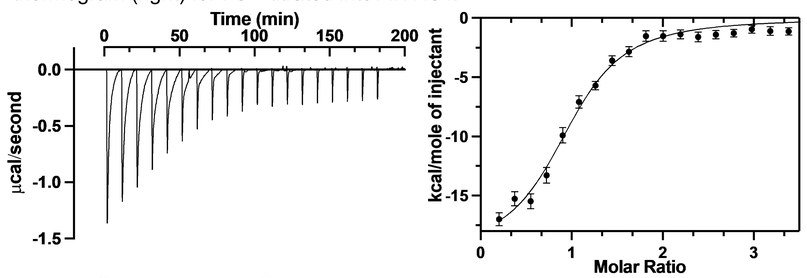

Table 2: Iron binding affinity, stoichiometry, and thermodynamic parameters measured for each chelator using ITC (n=3)

Fe Oxidation State	Compound	ITC K_d Value (µM)	Stoichiometry (Fe/Compound)	ΔG (kJ/mol)	ΔH (kJ/mol)	ΔS (J/mol•K)
Fe^{2+} (pH 7.5)	ATH434	4.60 ± 1.9	1.00 ± 0.5	-31.3 ± 1.7	-106.1 ± 1.5	-246.7 ± 0.7
	DFX	1.42 ± 0.5	0.24 ± 0.02	-34.0 ± 0.9	-59.6 ± 0.5	-84.5 ± 4.5
	DFP	13.9 ± 0.2	0.27 ± 0.2	-28.2 ± 0.1	-78.7 ± 1.9	-166.5 ± 6.4
	DMOG	19.6 ± 1.6	0.22 ± 0.04	-27.3 ± 0.2	-12.3 ± 1.3	49.5 ± 3.7
	IOX3	59.1 ± 3.9	0.34 ± 0.1	-24.5 ± 0.1	-79.3 ± 1.3	-180.6 ± 4.1
Fe^{3+} (pH 5.5)	ATH434	0.46 ± 0.04 [7]	1.4 ± 0.21	-36.8 ± 0.4	-53.3 ± 0.5	-54.4 ± 4.3
	DMOG	4.53 ± 1.4	1.53 ± 0.20	-31.9 ± 1.2	-120.8 ± 0.21	-293.2 ± 8.3
	IOX3	9.59 ± 0.13	0.85 ± 0.05	-17.49 ± 0.04	-21.04 ± 1.2	-11.6 ± 1.2

- ATH434's 1:1 stoichiometry (Fe^{2+} and Fe^{3+}) allows for intracellular iron-ligand exchange.
- ATH434 achieves thermodynamically favorable Fe^{2+} binding *via* strong enthalpic contributions, suggesting binding is significantly impacted by hydrogen bonding and van der Waals interactions.

Metal Site Structure Characterization

Figure 4: X-ray absorption near edge structure (XANES) of Fe^{2+} bound ATH434. A) Representative figure of the XANES spectrum of ATH434 with 1s-3d pre-edge transitions (B).

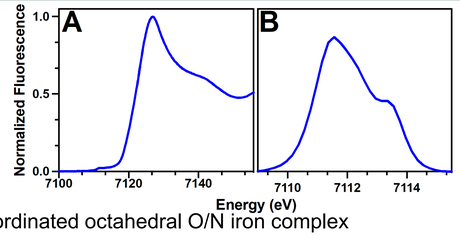

- Each compound forms a 6-coordinated octahedral O/N iron complex

Figure 5: ATH434-Fe^{2+} extended fine structure of the X-ray absorption spectrum (EXAFS). A) EXAFS spectrum and Fourier Transform (B) with empirical data in black and theoretical data in green.

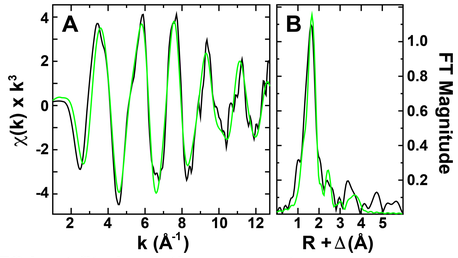

Table 4: EXAFS best fit simulation parameters

Fe Oxidation State	Compound	Atom	Bond Length (Å)	Coordination #	Bond Disorder
Fe^{2+}	ATH434	O/N	2.08	2	1.99
		O/N	2.20	3	3.80
	DFX	O/N	2.11	5.5	5.88
	DFP	O/N	2.12	5.5	5.63
	DMOG	O/N	2.11	6	5.61
	IOX3	O/N	2.04	1.5	3.33
		O/N	2.17	3	1.00
Fe^{3+}	ATH434	O/N	1.93	1	3.45
		O/N	2.09	3	4.72
	DMOG	O/N	1.97	2.5	3.00
		O/N	2.08	3.5	4.58
	IOX3	O/N	1.96	3	1.58
		O/N	2.10	2.5	1.56

- Each compound coordinates iron using O/N nearest neighbor ligands

Conclusions

The unique iron binding properties of ATH434 suggests this drug could be suited to assist in intracellular iron targeting and delivery. These novel properties include:

- Low micromolar binding affinity for intracellular Fe^{2+}, similar to endogenous iron chaperones including FXN and PCBP [1-3]
- Sub-micromolar affinity for Fe^{3+}, significantly weaker than that of traditional chelators DFX and DFP [5-6], allowing for selective targeting of pathogenic Fe^{2+}
- 1:1 Fe^{2+} stoichiometry, a coordination architecture that would allow for the recognition and drug-protein exchange of Fe^{2+} bound ATH434

Proposed Structure of ATH434 Bound to Intracellular Fe^{2+}

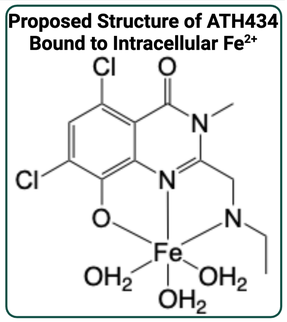

References

1. Cook, Jeremy D et al. "Monomeric yeast frataxin is an iron-binding protein." Biochemistry vol. 45,25 (2006): 7767-77. doi:10.1021/bi060424r
2. Bou-Abdallah, Fadi et al. "Iron binding and oxidation kinetics in frataxin CyaY of Escherichia coli." Journal of molecular biology vol. 341,2 (2004): 605-15. doi:10.1016/j.jmb.2004.05.072
3. Shi, H et al. "A cytosolic iron chaperone that delivers iron to ferritin." Science vol. 320 (2008): 1207-1210. doi:10.116/science.1157643
4. Pandolfo, Massimo et al. "Deferiprone in Friedreich ataxia: a 6-month randomized controlled trial." Annals of neurology vol. 76,4 (2014): 509-21. doi:10.1002/ana.24248
5. Steinhauser, Stefan et al. "Complex Formation of ICL670 and Related Ligands with Fe^{III} and Fe^{II}." Eur. J. Inorg. Chem., (2004): 4177-4192. doi:10.1002/ejic.200400363
6. Nurchi, Valeria M et al. "Potentiometric, spectrophotometric and calorimetric study on iron(III) and copper(II) complexes with 1,2-dimethyl-3-hydroxy-4-pyridinone." Journal of inorganic biochemistry vol. 102,4 (2008): 684-92. doi:10.1016/j.jinorgbio.2007.10.012
7. The ATH434 Apparent K_d at pH 5.5 (K_d/f_L) is consistent with that previously reported (Finkelstein, D.I. DOI 10.1186/s40478-017-0456-2, App K_d of $10^{-9.55}$ (~0.3 nM) at 7.4) when corrected for the lower fraction of ionized ligand (f_L $10^{-4.66}$ @ pH 5.5 vs $f_L 10^{-2.31}$ @ pH 7.4)